THE PUBLISHING HOUSE
OF THE ROMANIAN ACADEMY

PROCEEDINGS OF THE ROMANIAN ACADEMY, Series A,
Volume 17, Number 4/2016, pp. 344–351

ON WORKSPACE AND ACCURACY EVALUATION OF A PARALLEL ROBOT FOR NEEDLE PLACEMENT PROCEDURES

Bogdan GHERMAN, Doina PISLA, Calin VAIDA, Nicolae PLITEA

Technical University of Cluj-Napoca, Romania
Corresponding author: Doina Pisla, E-mail: doina.pisla@mep.utcluj.ro

Abstract. Needle placement is an important procedure in many medical fields, especially in diagnosis (for the achievement of biopsies) or cancer treatment procedures (like brachytherapy). The paper presents an extensive study of the workspace for an innovative parallel robot designed for needle placement procedures. The singularities of the parallel robot are exhaustively analysed and the possibilities of avoiding them are described. A study regarding the positioning and orientation accuracy and the influence of each active joint upon the end-effector (needle) is achieved.

Key words: workspace, singularities, parallel robot, accuracy, needle placement.

1. INTRODUCTION

The concept of minimally invasive interventions is spreading in all major fields of medicine, mainly due to the advantages it brings to the patient: faster recovery, less blood loss, improved aesthetics. There are medical cases when the minimal invasive procedure is the only way to treat certain diseases, like advanced stages of cancer, especially in hard-to-reach areas and when patients will not withstand classic surgery-based interventions due to their frailty. The field of application for the robotic structure studied in this paper refers to general placement procedures in the fields like brachytherapy or biopsy of different internal organs, for cancer treatment. Brachytherapy (BT) involves the placement of tiny radioactive seeds in a pre-arranged form into the tumor and are left there for a certain time or even discarded there [1], in order to irradiate only the tumorous cells and without affect the healthy tissue. In [2], the author demonstrates that a robotic device enhances the needle placement accuracy beyond the natural human capabilities. This is an important aspect that motivates the development of such devices, especially since the use of a robot can extend the applications of this technique. Several robotic systems have already been developed for BT [3, 4, 5, 6, 7], most of them just for prostate cancer BT treatment. In [8] and [9] have been developed modular robotic structures for general BT procedures, both having 5 DOF, enough for the intended application. Other systems can be studied, improved and adapted for needle placement procedures [10, 11, 12, 13]. Podder *et al*. In [14] have proved that most of the developed robotic systems for BT have been designed for prostate cancer treatment, underlying the need of developing new robotic solutions able to reach larger areas of the body, especially the deeply located tumors for which a manual procedure would be impossible.
The paper presents a workspace analysis of an innovative parallel robotic structure [15] designed for needle placement procedures. The singular configurations of the robot are obtained in an analytical form, while a solution for their avoidance is given in each case. The influence of each active joint upon the position and orientation of the needle is also assessed.

2. THE GEOMETRIC MODEL OF THE ROBOT

The robot (Fig. 1) consists of two parallel modules, each having $M = 3$ degrees of freedom (DOF), the first one (CYL-U) with three active joints (q_1, q_2, q_3), working in cylindrical coordinates, and the second one with two active joints (q_4, q_5), the modules being positioned at a known distance d_x. The active joints q_1 and

q_2 translate along an axis parallel with the OZ axis of the robot, while q_3 is an active joint rotating around the same axis. The joints q_4 and q_5 translate in the *YOZ* plane, with q_4 translating along the OZ axis and q_5 along the O*Y* axis of the foxed frame of the robot.

The geometric model has been presented in [15] in detail, therefore in this paper the authors will outline only the final equations that will lead to the study of the singular configurations. The geometrical parameters of the robot are: $d,b,c,l_1,l_2,l_3,l_c,h.,d_x,e$. Equation (1) describes the *inverse geometrical model* of the robot (q_1,q_2,q_3,q_4,q_5):

$$\begin{aligned}
q_1 &= Z_E + (h + l_c)\cdot\cos(\theta) + l_1 \\
q_2 &= q_1 + \sqrt{d^2 - (r_A - b)^2} \\
q_3 &= \pi - a\tan 2\left(Y_E - (h + l_c)\cdot\sin(\theta)\cdot\sin(\psi), d_x - X_E + (h + l_c)\cdot\sin(\theta)\cdot\cos(\psi)\right). \\
q_4 &= Z_E + h\cdot\cos(\theta) - l_2 \\
q_5 &= Y_E - h\cdot\sin(\theta)\cdot\sin(\psi) - \sqrt{c^2 - \left(X_E - h\cdot\sin(\theta)\cdot\cos(\psi)\right)^2}
\end{aligned} \tag{1}$$

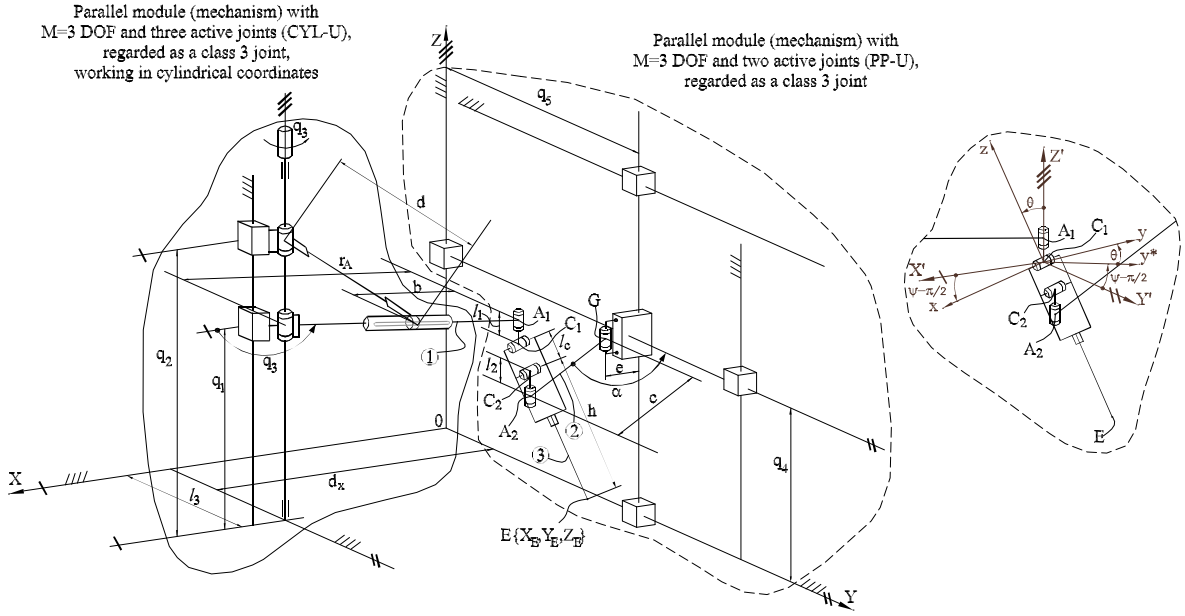

Fig. 1 – Kinematic scheme of the parallel robot for needle placement.

The *direct geometric model* of the robot yields two solutions, mainly from solving the following system of equations:

$$\begin{cases} (Y_{A2} - Y_{A1})^2 + (X_{A2} - X_{A1})^2 = l_c^2 - (Z_{C1} - Z_{C2})^2 \\ X_{A2}^2 + (Y_{A2} - q_5)^2 = c^2 \end{cases} \tag{2}$$

from where two possibilities for the coordinates of point A_2 are obtained. Both equations of the system (2) are circle equations in a plane parallel to the *XOY* plane: the first one has the center in point A_1 and the radius $\sqrt{l_c^2 - (Z_{C1} - Z_{C2})^2}$ and the second one with the center in point *G* and radius *c*. The other members of the equation (2) are known:

$$\begin{aligned}
X_{A1} &= d_x - r_A\cdot\cos(\pi - q_3) \\
Y_{A1} &= r_A\cdot\sin(\pi - q_3) \\
Z_{A1} &= q_1
\end{aligned} \tag{3}$$

The coordinates of point $E(X_E, Y_E, Z_E)$ are:

$$\begin{aligned} X_{E\_i} &= X_{C1} + (h + l_c)\cdot \sin(\theta)\cdot \cos(\psi_i) \\ Y_{E\_i} &= Y_{C1} + (h + l_c)\cdot \sin(\theta)\cdot \sin(\psi_i) \quad , i = 1..2 \\ Z_E &= Z_{C1} - (h + l_c)\cdot \cos(\theta) \end{aligned} \tag{4}$$

and

$$\begin{aligned} \psi_i &= a\tan 2\left(Y_{A2\_i} - Y_{A1}, X_{A2\_i} - X_{A1}\right), \qquad i = 1..2 \\ \theta &= a\tan 2\left(\sqrt{l_c^2 - (Z_{C1} - Z_{C2})^2}, (Z_{C1} - Z_{C2})\right) \end{aligned} \tag{5}$$

3. SINGULARITY ANALYSIS

Kinematic singularities represent one of the main concerns in the design parallel robots. A parallel robot in a singular configuration either loses or gains one or more degrees of freedom instantaneously, losing its designated motion and working capabilities. Therefore, in the design stage of the medical robot, singularities must be eliminated from the workspace of the robot or acknowledged and avoided in the robot control. Ma and Angeles in [16] classified the singularities into three categories: *architecture*, *configuration* and *formulation* singularities. The most studied category is the configuration singularities. Gosselin and Angeles in [17] and Tsai in [18] classified singularities into three main groups, based on the properties of the Jacobian matrices of the closed-loop mechanism, the relation that describes the connection between the vectors of the end-effector velocity ($\dot{X}$) and the active-joint velocity ($\dot{q}$) being written as:

$$A\dot{X} = -B\dot{q}\,, \tag{6}$$

where A and B are the Jacobian matrices of the closed-loop mechanism. When matrix B is singular, first type singularities occur and the robot reaches configurations in which it loses one or more degrees of freedom. When matrix A is singular (second type singularities), the parallel manipulator gains one or more degrees of freedom and it becomes uncontrollable. When both matrices are simultaneously singular, the third type of singularities occurs, the so-called architectural singularities that can be usually avoided in the design stage.

The robot Jacobian is written in the form presented in (7), from which the two matrices A and B are obtained:

$$\begin{aligned} &f_1(Z_E, \theta, q_1) \equiv Z_E + (h + l_c)\cdot \cos(\theta) + l_1 - q_1 = 0 \\ &f_2(X_E, \psi, \theta, q_1, q_2, q_3) \equiv X_E + (h + l_c)\cdot \sin(\theta)\cdot \cos(\psi) - d_x + \left(b - \sqrt{d^2 - (q_2 - q_1)^2}\right)\cdot \cos(\pi - q_3) = 0 \\ &f_3(Y_E, \psi, \theta, q_1, q_2, q_3) \equiv Y_E + (h + l_c)\cdot \sin(\theta)\cdot \sin(\psi) - \left(b - \sqrt{d^2 - (q_2 - q_1)^2}\right)\cdot \sin(\pi - q_3) - l_3 = 0 \\ &f_4(Z_E, \theta, q_4) \equiv Z_E - l_2 + h\cdot \cos(\theta) - q_4 = 0 \\ &f_5(X_E, Y_E, \psi, \theta, q_5) = (X_E - h\cdot \sin(\theta)\cdot \cos(\psi) - e)^2 + (Y_E - h\cdot \sin(\theta)\cdot \sin(\psi) - q_5)^2 - c^2 \end{aligned} \tag{7}$$

3.1. Type 1 singularities

These types of singularities occur when $\det(B) = 0$. The determinant has been computed and has the following form:

$$\det(B) = 2\cdot (q_5 - Y_E + h\cdot \sin(\psi)\cdot \sin(\theta))\cdot \frac{\sqrt{d^2 - (q_2 - q_1)^2} + b}{\sqrt{d^2 - (q_2 - q_1)^2}}\cdot (q_2 - q_1). \tag{8}$$

Four cases in which the determinant becomes null are distinguished:

1. $\sqrt{d^2 - (q_2 - q_1)^2} = 0$ when the determinant cannot be computed. This configuration means that the element having the length d is parallel to the OZ axis (and the distance between the active joints q_1 and q_2 is d). In this case, the robot (and more precisely the CYL-U module) is blocked. This

could be easily avoided by imposing the maximum distance between the two active joints (in robot control), so that $q_2 > q_1$.

2. $q_5 - Y_E + h \cdot \sin(\psi) \cdot \sin(\theta) = 0$, or knowing that $Y_{A2} = Y_E - h \cdot \sin(\psi) \cdot \sin(\theta)$, this case could be written as $q_5 - Y_{A2} = 0$. This position is illustrated in figure 2, and it occurs when the angle $\alpha = \frac{\pi}{2}$, with $\alpha = a\tan 2(Y_{A2} - q_5, X_{A2} - e)$. This type of singularity could also be avoided by imposing in the robot control the following condition: $q_5 < Y_{A2}$.

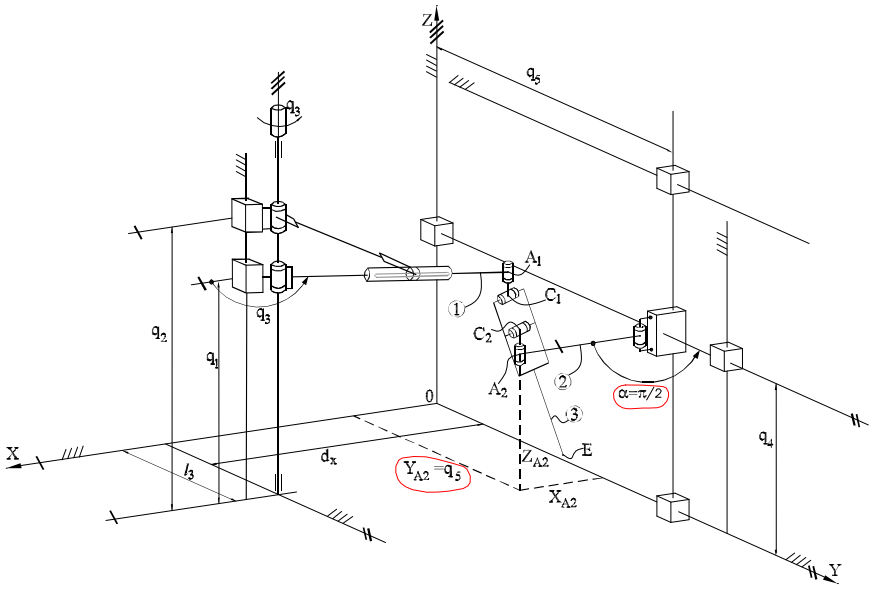

Fig. 2 – Schematic representation of the singularity of type 1 – case no. 2.

3. $\sqrt{d^2 - (q_2 - q_1)^2} + b = 0$, which might happen only if all three expressions are zero, since each represent always positive quantities. This singularity can be avoided since the design stage, imposing that $b > 0$ (Fig. 1).
4. $q_2 - q_1 = 0$, which could be avoided if the condition at number 1 ($q_2 > q_1$) is imposed.

3.2. Type 2 singularities

These types of singularities occur when $\det(A) = 0$. The determinant has been computed and has the following form:

$$\det(A) = 2 \cdot l_c^2 \cdot \sin^2(\theta) \cdot \left((X_E - e) \cdot \sin(\psi) - (Y_E - q_5) \cdot \cos(\psi)\right). \tag{9}$$

In this case, the robot gains one or more DOF and three cases can be distinguished:

5. $\sin(\theta) = 0$, meaning that $\theta = 0$ or $\theta = \pi$. The second case, when $\theta = \pi$ is not plausible in real-life, since the patient and tumor is always situated below the robot, so the needle will not usually go upwards, at an angle $\theta > \frac{\pi}{2}$ (and never at $\theta = \pi$). The first case ($\theta = 0$) is highly possible and has to be considered and avoided in the robot control. The source of this singularity consists in the use of the two passive Cardan joints, whose first rotation axis is vertical, meaning that the needle will move freely around its symmetry axis. This configuration is illustrated in Fig. 3.
6. $(X_E - e) \cdot \sin(\psi) - (Y_E - q_5) \cdot \cos(\psi) = 0$. If $\psi \neq \frac{\pi}{2}$, it yields:

$$\tan(\psi_2) = \frac{Y_E - q_5}{X_E - e} \tag{10}$$

Considering that the orientation angle ψ can be computed in the following way:

$$\tan(\psi)=\frac{Y_E-Y_{A2}}{X_E-X_{A2}}. \tag{11}$$

From figure 4, it is easy to see that the angle ψ (from (11)) becomes equal to ψ_2 (from (10)) when element c is collinear with the segment GE', where E' represents the projection of point E on the XOY plane (the same goes for points C_1' and C_2').

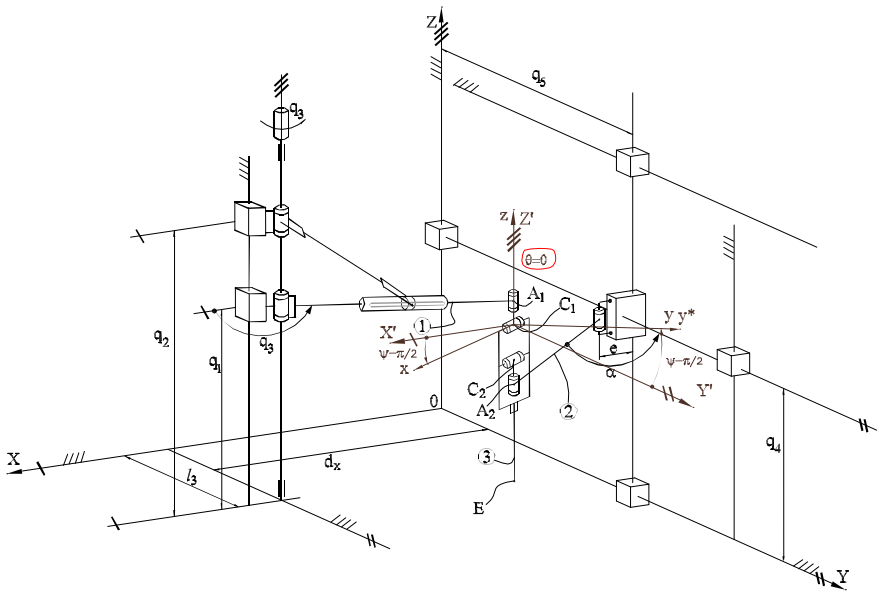

Fig. 3 – Schematic representation of the singularity of type 2 – case no. 5.

The plane defined by the points G, E and E' is a separation plane between two working modes of the robot, as it can be observed from solving the direct geometric model (when two solutions are obtained for the same active joints coordinates). Since the case when the element 2 (having the length c) being in the separation plane represents a singularity configuration (and subsequently the robot gains supplementary DOF), the robot becoming incontrollable, such positions must be avoided.

This configuration of the robot is presented in figure 5. In this case, the angle α (between the element 2, having the length c and the YOZ plane and computed as: $\alpha = a\tan 2\left(\frac{X_{A2}-e}{Y_{A2}-q_5}\right)$) becomes $\frac{\pi}{2}-\psi$.

If $\psi=\frac{\pi}{2}$, this singularity becomes a particular case when the links having the lengths c (element 2) and l_c are in the same plane and $X_E=e$ (or $\alpha=0$). This particular case can be avoided since the design stage, imposing the following restriction: $r_{A1}<d_x-e$.

4. ACCURACY ASSESSMENT

Accuracy assessment is a good example in needle placement procedures and brachytherapy, the target points being established prior to the actual needle insertion, using visual instruments, like the computer tomography, ultrasound or magnetic resonance. Therefore an important feature of robots designed for needle placement procedure consists in their positioning accuracy, which should not exceed 1 mm inside the human body [19]. This means that a good kinematic accuracy is needed, along with the proper selection of actuators. Liu and Wang in [20] have used a general method to evaluate the kinematic errors of parallel manipulators. In this sense, the robot has been placed in such a position that large enough amplitudes of motion can be achieved without intersecting singularity areas. For this position, the inverse geometric model has been used to determine the active joint coordinates (q_1, q_2, q_3, q_4, q_5). Further, each active joint has been individually

incremented with a predefined value ($\varepsilon = 0.05$ mm) and for each new value, using the direct geometric model, the needle tip coordinates (X_E, Y_E, Z_E) and its orientation (the angles ψ and θ) have been determined.

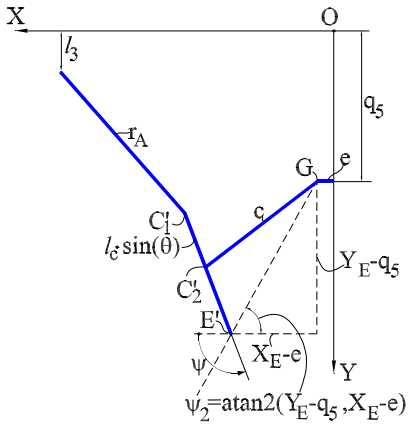

Fig. 4 – Schematic representation of the singularity of type 2 – case no. 6 –projections on the *XOY* plane.

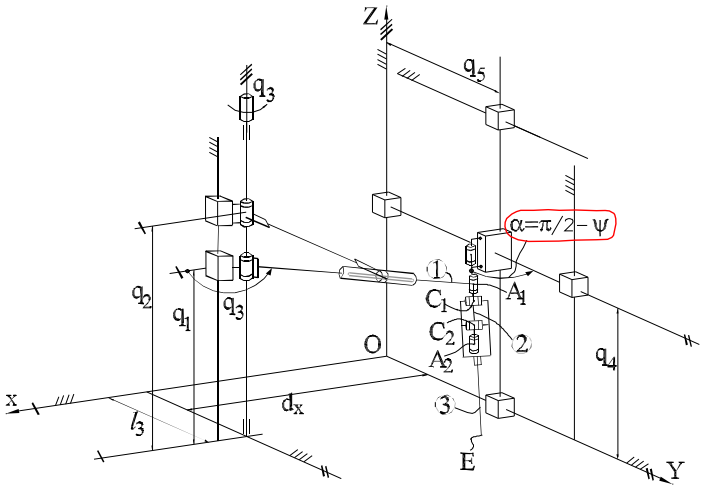

Fig. 5 – Schematic representation of the robot configuration singularity of type 2 – case no. 6.

At each step (i-th iteration), the position and orientation variation have been recorded:

$$\text{pos\_err}_i = \sqrt{\left(X_{E_i} - X_{E_{i-1}}\right)^2 + \left(Y_{E_i} - Y_{E_{i-1}}\right)^2 + \left(Z_{E_i} - Z_{E_{i-1}}\right)^2} \tag{12}$$

$$\psi\_err_i = \psi_i - \psi_{i-1} \tag{13}$$

$$\theta\_err_i = \theta_i - \theta_{i-1}. \tag{14}$$

This is a simple way to observe the influence of each active joint upon the robot position (pos_err_i) and its orientation (ψ _ err_i and θ _ err_i). Figure 7 presents the needle tip positioning (X, Y, Z) variation with the variation of the first (q_1) active joint, providing information about influence of this joint upon the motion resolution of the end-effector. The maximum resolution is obtained when this joint is between 380 and 440 mm, with a minimum of 0.125 mm at a constant variation of the joint of ε = 0.05 mm, leading to a ratio $n = 5$. This aspect is mainly due to the length of the robotic rods (elements *b*, *d* and *c*). Figure 8 presents the variation of the orientation angle θ in degrees, with the variation of the q_1 active joint. A minimum is registered at around 380–390 mm (again) with the value of 0.0286^0. Things are similar for the ψ angle.

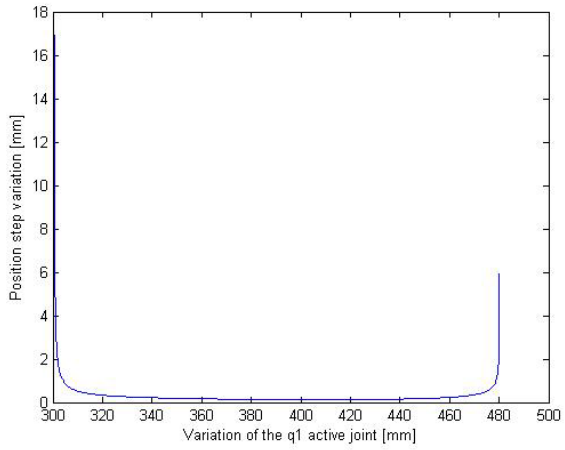

Fig. 7 – Position variation of the needle tip (*X*, *Y*, *Z*) with the variation of the q_1 active joint.

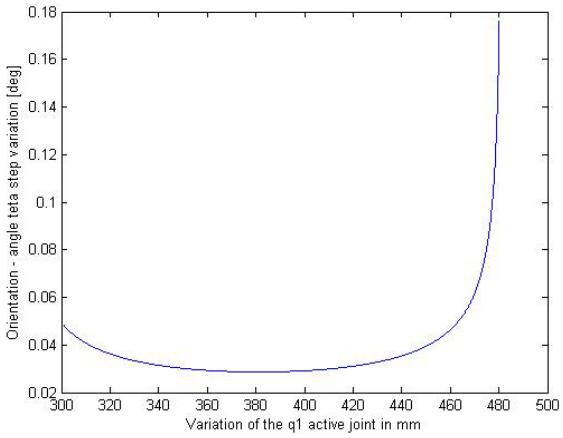

Fig. 8 – Position variation of the needle orientation (angle θ) with the variation of the q_1 active joint.

For the second active joint (q_2) the maximum resolution is $2.6 \cdot 10^{-6}$, with the ratio $n = 5.244 \cdot 10^{-5}$ (Fig. 9 presents the position variation of the needle tip which is smaller than the input joint variation). An interesting fact is that the orientation angle θ is not influenced by this joint (Fig. 10).

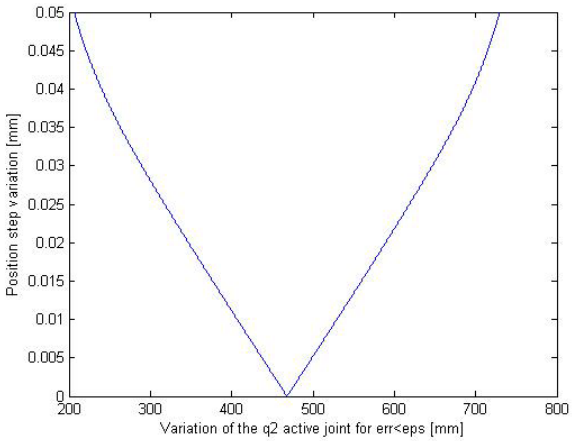

Fig. 9 – Position variation of the needle tip (*X*, *Y*, *Z*) smaller than the variation of the q_2 active joint (ε = 0.05 mm).

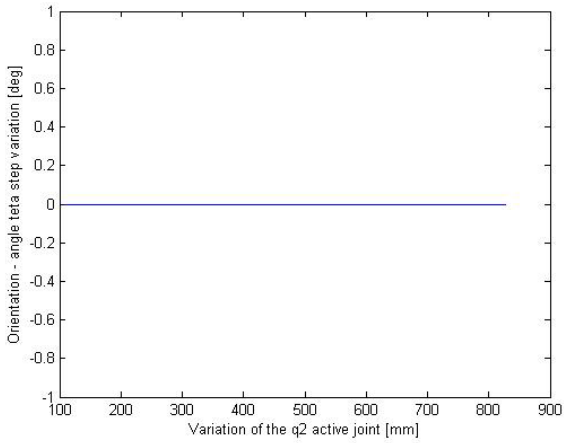

Fig. 10 – Orientation angle θ keeps constant value with the variation of the q_2 active joint.

Figure 11 presents the needle tip variation with the variation (in degrees) of the active joint q_3. At an input of $\varepsilon = 0.05^\circ$, the maximum positioning resolution is of 1.22 mm, again due to the geometric parameters of the robot *d* and *b*. Figure 12 shows that this active joint (q_3) does not influence the θ orientation angle. Similar results are obtained for the other two active joints: q_4 influences both the position and orientation of the needle, while q_5 influences only the position of the needle tip and the ψ orientation angle.

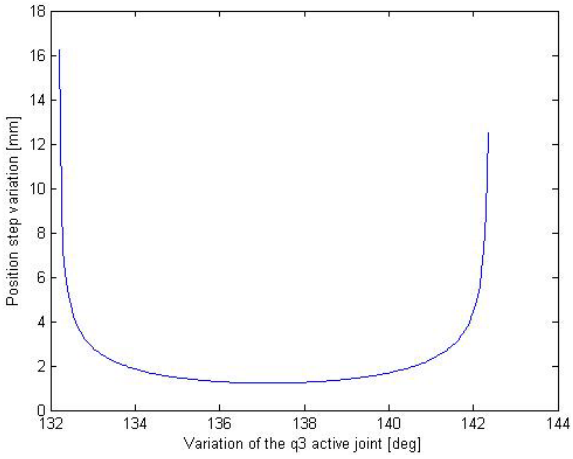

Fig. 11 – Position variation of the needle tip (*X*, Y, *Z*) with the variation of the q_3 active joint.

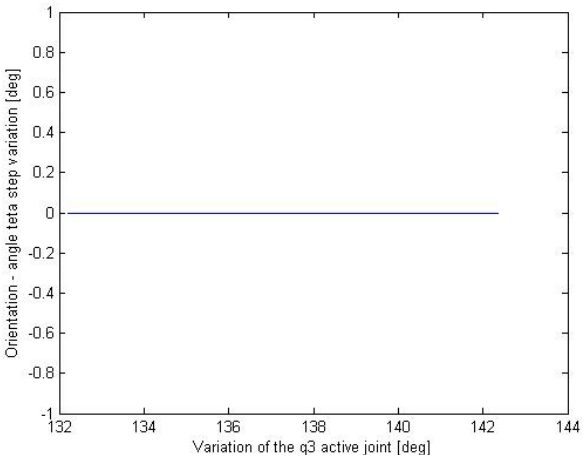

Fig. 12 – Orientation angle θ keeps constant value with the variation of the q_3 active joint.

5. CONCLUSIONS

The paper presents the workspace analysis of a parallel robot designed for needle placement procedures, especially brachytherapy. The singularities of this robot have been studied and presented, in an analytical way, while some solutions for avoiding them in the robot control have been suggested. Based on the geometric model of the robot, two working areas have been determined, separated by a singular configuration. A study concerning the accuracy assessment and the influence of each active joint upon the position and orien-

tation of the needle has been achieved. The ratio input(ε)/output(position [mm] and orientation [deg]) proves that the selection of the motors and transmission mechanisms is crucial for accomplishing the required tasks for an accurate needle insertion.

ACKNOWLEDGEMENTS

This paper was realized within the project financed from the European Social Fond through POSDRU program, DMI 1.5, ID 137516-PARTING (for the first author), the Partnership Programme in priority domains – PN-II, which runs with the financial support of MEN-UEFISCDI, Project no. 247/2014, the Project no. 173/2012, code PN-II-PCCA-2011-3.2-0414, entitled ”Robotic assisted brachytherapy, an innovative approach of inoperable cancers - CHANCE” financed by UEFISCDI .

REFERENCES

1. GERBAULET A., PÖTTER R., MAZERON J-J., MEERTENS H., LIMBERGEN E.V., *The GEC ESTRO handbook of brachytherapy*, Eur. Soc. for Ther. Rad. and Onc. Leuven, Belgium, 2002.
2. MATEESCU D., *Oncology patient guide*, Bennet Publishing House, Bucharest, 2010.
3. YU Y., PODDER T., ZHANG Y., NG W.S., MISIC V., SHERMAN J., FU L., FULLER D., MESSING E., *Robot-Assisted Prostate Brachytherapy*, Proc. Med. Img. Comp. and Comp.-Assist. Interv., Springer-Verlag, Berlin, 2006, pp. 41–49.
4. ZHANG Y.D., PODDER T.K., NG W.S., SHERMAN J., MISIC V., FULLER D., MESSING E., *Semi-automated Needling and Seed Delivery Device for Prostate Brachytherapy*, Proc. on Int. Rob. and Sys., IEEE, Beijing, 2006, pp. 1279–1284.
5. SONG D.Y., BURDETTE E.C., FIENE J., ARMOUR E., KRONREIF G., DEGUET A., *Robotic needle guide for prostate brachytherapy*, Brachytherapy, **10**, pp. 57–63, 2011.
6. DE LESO P.B., MULLASSERY V., SHRIMALI R., LOWE G., BRYANT L., HOSKIN P.J., *Image-guided vulvovaginal interstitial brachytherapy in the treatment of primary and recurrent gynecological malignancies*, Brachytherapy, **11**, *4*, pp. 306–10, 2011.
7. JIANG S.,GUO J., LIU S., LIU J., YANG J., *Kinematic analysis of a 5-DOF hybrid-driven MR compatible robot for minimally invasive prostatic interventions*, Robotica, **30**, ***7***, pp. 1147–1156, 2010.
8. PLITEA N., PISLA D., VAIDA C., GHERMAN B., SZILAGHYI A., GALDAU B., COCOREAN D., COVACIU F., *On the Kinematics of a New Parallel Robot for Brachytherapy*, Proceedings of the Romanian Academy – series A: Mathematics, **15**, *4*, pp. 354–361, 2014.
9. PLITEA N., SZILAGHYI A., PISLA, D., *Kinematic Analysis of a new 5-DOF Modular Parallel Robot for Brachytherapy*, Robotics and Computer Integrated Manufacturing, **31**, pp. 70–80, 2015.
10. TARNITA D., MARGHITU D., *Analysis of a hand arm system*, Robotics and CIM, **29**, 6, pp. 493–501, 2013.
11. OTTAVIANO E., VOROTNIKOV S., CECCARELLI M., KURENEV P., *Design improvements and control of a hybrid walking robot*, Robotics and Autonomous Systems, **59**, pp. 128–141, 2011.
12. PISLA D., GHERMAN B., VAIDA C., SUCIU M., PLITEA N., *An active hybrid parallel robot for minimally invasive surgery*, Robotics and CIM, **29**, *4*, pp. 203–221, 2013.
13. STAICU S., *Recursive modelling in dynamics of Agile Wrist spherical parallel robot*, Robotics and CIM, **25**, pp. 409–416, 2009.
14. PODDER T.K., BEAULIEU L., CALDWELL B., *et al*., *AAPM and GEC-ESTRO guidelines for image-guided robotic brachytherapy: report of Task Group 192*, Med Phys., **41**, *10*, 2014.
15. GHERMAN B., PLITEA N.,VAIDA C., PISLA D., *Kinematic Modelling of a new 5-DOF (Axis) Parallel Robot used in Brachytherapy*, Applied Mechanics and Materials, **762** (Mechatronics and Robotics), pp. 131–136, 2015.
16. MA O., ANGELES J., *Architecture singularities of platform manipulators*, Proceedings of IEEE Conference on Robotics and Automation, California, USA, April 1991, pp. 1542–1547.
17. GOSSELIN C., ANGELES J., *Singularity analysis of closed-loop kinematic chains*, IEEE Transactions on Robotics and Automation, **6**, *3*, pp. 281–290, 1991.
18. TSAI L.-W., *Robot Analysis*, John Wiley &Sons, 1999.
19. MCGILL C.S., SCHWARTZ J.A., MOORE J.Z., MCLAUGHLIN P.W., SHIH A.J., *Precision grid and hand motion for accurate needle insertion in brachytherapy*, Med. Phys., **38**, *8*, pp. 4749–59, 2011.
20. LIU X.-J., WANG J., *Parallel Kinematics Type, Kinematics, and Optimal Design*, Springer Tracts in Mechanical Engineering, pp. 196–199, 2014.

Received June 5, 2015